

https://dspace.org/

Performance Analysis of Digital Communication Systems over Fading Channels

Jules Mouatcho Moualeu; D da Costa; Walaa Hamouda; Ugo S. Dias; Rausley A. A de Souza

https://hdl.handle.net/10539/28030
ISI

Downloaded from a DSpace repository. https://dspace.org/

This article has been accepted for publication in a future issue of this journal, but has not been fully edited. Content may change prior to final publication. Citation information: DOI 10.1109/LCOMM.2018.2878218, IEEE Communications Letters

Performance Analysis of Digital Communication Systems over α-κ-μ Fading Channels

Jules M. Moualeu, *Senior Member, IEEE*, Daniel B. da Costa, *Senior Member, IEEE*, Walaa Hamouda, *Senior Member, IEEE*, Ugo S. Dias, *Senior Member, IEEE*, and Rausley A. A. de Souza, *Member, IEEE*

***Abstract*—In this letter, the performance of digital communications systems over α-κ-μ fading channels is analyzed in terms of outage probability, average channel capacity, and average error rate (AER) for a variety of modulation formats. To this end, novel and exact expressions for the aforementioned performance metrics are derived, based on which an asymptotic analysis is carried out. The derived expressions are valid for arbitrary values of the fading parameters, namely α, κ, and μ, and their accuracies are validated through Monte Carlo simulations.**

***Index Terms*—α-κ-μ fading model, average channel capacity, bit error rate, outage probability.**

I. Introduction

MOBILE communications are characterized by some phenomena including shadowing and multipath fading. Particularly, shadowing is relatively slow and gives rise to long-term signal variations, while multipath fading is due to constructive and destructive interferences as a result of delayed, scattered, diffracted and reflected signal components, and encompasses small-scale fading, i.e., Rayleigh, Weibull, Rician, and Nakagami-m [1]. In recent years, generalized fading models such as α-μ, κ-μ, η-μ, α-η-μ, α-κ-μ, and α-η-κ-μ have attracted a lot of interest due to their versatility and wide applicability in practical scenarios [2]–[6].

Owing to this fact, several research studies have been devoted to the performance analysis of wireless communication systems over generalized fading models [7]–[15]. In [7], novel closed-form expressions for the average channel capacity and bit-error rate (BER) were obtained. In [8], the outage performance of maximal-ratio combining (MRC) receivers in η-μ fading channels was studied. Novel expressions for the average channel capacity over η-μ and κ-μ fading were derived in [9], while the moment generating function (MGF) and average error rate (AER) were obtained in [10]. Similarly, studies were presented for the α-μ fading model in [11]. The work in [12] presented a comprehensive performance analysis for digital communication systems over generalized α-η-μ fading distribution. In [13], α-η-μ and α-κ-μ fading models were investigated in which more emphasis was given to the former model, with the α-κ-μ model being briefly examined. In that work, neither the exact outage probability (OP) was investigated nor an asymptotic analysis for the AER was carried out. Moreover, the derived metrics obtained were only valid for integer values of the fading parameter α. In [14], an analysis of the channel capacity of wireless communications that operate in the complex fading model, i.e., α-η-κ-μ fading model, was investigated. Although [14] provides a thorough analysis of the channel capacity of the generalized α-η-κ-μ fading channels, other metrics such as OP and AER were not studied. In contrast to [13] and [14], the work of [15] is twofold: (i) to show that the α-η-κ-μ fading model is the best fit for signal propagation in millimiter wave (mmWave) communications; (ii) to derive some higher-order statistics.

As aforementioned, the α-κ-μ fading models have recently gained in popularity since they can model a variety of realistic channel models. In light of this, it is important to provide in-depth studies under such fading conditions. Motivated by the above-cited limitations, a comprehensive and general performance analysis of digital communication systems over α-κ-μ fading channels is provided and we believe it will constitute an advancement and will be useful to future readers. Exact analytical expressions for the OP, average channel capacity, and AER of coherent modulation schemes, are obtained and are valid for arbitrary fading parameters values in contrast to [13]. Our derived expressions include single infinite series which converge rapidly and steadily after a few terms to ensure acceptable truncation that yields accurate results. To this end, simple closed-form bounds for the truncation error of the derived series representations are obtained. In addition, an asymptotic analysis is carried out and new insights related to the system diversity/array gains are highlighted. Finally, representative numerical examples are provided and verified through Monte Carlo simulations. To the best of the authors' knowledge, the results achieved in this work have not been reported in the literature yet.

II. The α-κ-μ Fading Model

The α-κ-μ is a generalized fading model which includes some well-known fading distributions, such as Rayleigh, Nakagami-m, Weibull, one-sided Gaussian, Rician and κ-μ, as special cases. By denoting γ as the instantaneous signal-to-noise ratio (SNR), and applying probability theory and [16, Eq. (8.445.1)] in [4, Eq. (6)], the probability density function (PDF) of γ can be written in its infinite series representation as

$$f_\gamma(x) = \sum_{j=0}^{\infty} \frac{\alpha \mu^{\mu+2j} \kappa^j \left(1+\kappa\right)^{\mu+j}}{2\Gamma(\mu+j) j! e^{\kappa\mu} \bar{\gamma}^{\frac{\alpha}{2}(\mu+j)}} x^{\frac{\alpha}{2}(\mu+j)-1} e^{-\frac{\mu(1+\kappa)}{\bar{\gamma}^{\frac{\alpha}{2}}} x^{\frac{\alpha}{2}}}, \tag{1}$$

J. M. Moualeu is with the School of Electrical and Information Engineering, University of the Witwatersrand, Johannesburg, 2000, South Africa (e-mail: jules.moualeu@wits.ac.za).

D. B. da Costa is with the Department of Computer Engineering, Federal University of Ceará, Sobral, CE, Brazil (e-mail: danielbcosta@ieee.org).

W. Hamouda is with the Department of Electrical and Computer Engineering, Concordia University, Montreal, QC H3G 1M8, Canada (e-mail: hamouda@ece.concordia.ca).

U. S. Dias is with the Department of Electrical Engineering, University of Brasília, DF, Brazil (e-mail: ugodias@ieee.org).

R. A. A. de Souza is with the National Institute of Telecommunications (Inatel), Santa Rita do Sapuca 37540-000, Brazil (e-mail: rausley@inatel.br).

1089-7798 (c) 2018 IEEE. Personal use is permitted, but republication/redistribution requires IEEE permission. See http://www.ieee.org/publications_standards/publications/rights/index.html for more information.

This article has been accepted for publication in a future issue of this journal, but has not been fully edited. Content may change prior to final publication. Citation information: DOI 10.1109/LCOMM.2018.2878218, IEEE Communications Letters

where $\alpha > 0$ is the parameter describing the nonlinearity of the medium, $\kappa > 0$ is the ratio between the total power of the dominant components and the total power of the scattered waves, $\mu > 0$ denotes the total number of multipath clusters, and $\bar{\gamma}$ is the average SNR. Such a fading distribution includes the general κ-μ, Rayleigh, Nakagami-m, Rice, Weibull and one-sided Gaussian distributions. By setting $\alpha = 2$, the κ-μ distribution can be obtained. From the κ-μ distribution, the Nakagami-m, Rayleigh and one-sided Gaussian distributions can be obtained by letting $\kappa \to 0$ and varying the parameter $\mu = m$, $\mu = 1$, and $\mu = \frac{1}{2}$, respectively. The Rice distribution can be obtained from the κ-μ distribution by setting $\kappa = k$ and $\mu = 1$, while the Weibull distribution stems from the κ-μ one by setting $\kappa \to 0$ and $\mu = 1$.

III. Outage Probability

A. Exact OP

From (1), the OP can be formulated as $\mathcal{P}_{\text{out}} = \int_0^{\gamma_{\text{th}}} f_\gamma(x)\mathrm{d}x$, where $\gamma_{\text{th}} = 2^{R_{\text{th}}} - 1$ denotes the SNR threshold and R_{th} is the corresponding target transmission rate. With the aid of [16, Eq. (3.381.8)] and after some manipulations, the exact OP can be derived as

$$\mathcal{P}_{\text{out}} = \sum_{j=0}^{\infty} \frac{\mu^j \kappa^j}{j!\Gamma(\mu+j)e^{\kappa\mu}} \Upsilon\left(\mu + j, \frac{\mu(1+\kappa)}{\bar{\gamma}^{\frac{\alpha}{2}}}\gamma_{\text{th}}^{\frac{\alpha}{2}}\right), \quad (2)$$

where $\Upsilon(\cdot,\cdot)$ denotes the lower incomplete Gamma function [16, Eq. (8.354.1)].

B. Asymptotic OP

In order to gain further insights from (2), an asymptotic expression (i.e., at high-SNR regime) for the OP is now derived. Firstly, note that for large values of $\bar{\gamma}$, the term $j = 0$ of the infinite series dominates. In addition, using the following approximation $\Upsilon(a, x) \approx \frac{x^a}{a}$ for sufficiently low values of x, and after performing some manipulations, (2) can be asymptotically approximated by

$$\mathcal{P}_{\text{out}}^{\infty} \simeq \frac{\mu^{\mu-1}(1+\kappa)^\mu \gamma_{\text{th}}^{\frac{\alpha\mu}{2}}}{\Gamma(\mu)e^{\kappa\mu}} \bar{\gamma}^{-\frac{\alpha\mu}{2}}. \quad (3)$$

Interestingly, it is noteworthy that the diversity gain only depends on the nonlinearity parameter α and the number of multipath clusters μ (i.e., it does not depend on κ), whereas the array gain is dependent on all the fading parameters.

IV. Error Rate Analysis

A. Exact AER

Assuming coherent modulation schemes, the AER can be formulated as

$$\bar{\mathcal{P}}_e = A \int_0^{\infty} \text{erfc}\left(\sqrt{Bx}\right) f_\gamma(x)\mathrm{d}x, \quad (4)$$

where A and B are constant values depending on the modulation scheme, and $\text{erfc}(\cdot)$ denotes the complementary error function. From (1), knowing that $\text{erfc}\left(\sqrt{Bx}\right) = \frac{1}{\sqrt{\pi}} G_{1,2}^{2,0}\left(Bx \middle| \begin{matrix} 1 \\ 0, \frac{1}{2} \end{matrix}\right)$, where $G_{p,q}^{m,n}\left(\cdot \middle| \begin{matrix} \cdot \\ \cdot \end{matrix}\right)$ stands for the Meijer's G-function [16, Eq. (9.301)], relying on [17, Eq. (8.4.3.1)], after some manipulations, and with the aid of [18], an analytical expression for $\bar{\mathcal{P}}_e$ can be derived as (5), shown at the top of the next page, where $H_{p,q}^{m,n}\left(\cdot \middle| \begin{matrix} \cdot \\ \cdot \end{matrix}\right)$ is the Fox H-function defined in [17, Eq. (8.3.1)][1]. It is worthwhile to say that, although (5) is written in terms of an infinite sum, it converges quickly, requiring therefore in practice the evaluation of few number of terms to get an accuracy of 10^{-5}.

B. Asymptotic AER

In order to gain further insights into system parameters at high-SNR regime, an asymptotic analysis for the AER is carried out. By setting $\bar{\gamma} \to \infty$, the term $j = 0$ dominates in (1). Then, making use of the following approximation $e^{-\frac{1}{x}} \approx 1 - \frac{1}{x}$ as $x \to \infty$ in (1), and replacing the resulting expression in (4), the AER can be asymptotically approximated by

$$\bar{\mathcal{P}}_e^{\infty} \simeq \frac{\alpha A \mu^\mu (1+\kappa)^\mu}{2\Gamma(\mu)e^{\kappa\mu}\bar{\gamma}^{\frac{\alpha\mu}{2}}} \int_0^{\infty} \text{erfc}\left(\sqrt{Bx}\right) x^{\frac{\alpha}{2}-1}\mathrm{d}x. \quad (6)$$

To evaluate the integral in (6), the following identity is used: $\text{erfc}(\sqrt{Bx}) = \Gamma\left(\frac{1}{2}, Bx\right)$. Therefore, the resulting expression can be evaluated with the help of [16, Eq. (6.455.1)] and ${}_2F_1(a, b, c; 0) = 1$, and the resulting asymptotic expression for the AER can be attained as

$$\bar{\mathcal{P}}_e^{\infty} \approx \frac{A\mu^{\mu-1}(1+\kappa)^\mu \Gamma\left(\frac{1}{2}(\alpha+\mu)\right)}{\sqrt{\pi}\Gamma(\mu)e^{\kappa\mu}B^{\frac{\alpha\mu}{2}}} \bar{\gamma}^{-\frac{\alpha\mu}{2}}, \quad (7)$$

which shows a similar diversity gain as previously obtained for the outage probability. As well-known, for binary phase-shift keying (BPSK) modulation scheme, we have that $A = \frac{1}{2}$ and $B = 1$. Then, by substituting these values into (7) and considering Rayleigh fading (i.e., $\alpha = 2$, $\kappa \to 0$ and $\mu = 1$), the asymptotic AER reduces to $\bar{\mathcal{P}}_e^{\infty} \approx \frac{1}{4\bar{\gamma}}$ [20, p. 818].

V. Normalized Average Capacity

The normalized average channel capacity $\bar{\mathcal{C}}$ can be mathematically formulated as

$$\bar{\mathcal{C}} = \frac{1}{\ln 2} \int_0^{\infty} \ln(1+x) f_\gamma(x)\mathrm{d}x. \quad (8)$$

By substituting (1) in (8) yields an integrand which is a combination of a logarithm function and an exponential function having a more complicated argument, and therefore cannot be easily evaluated. To solve this inconvenience, we express both logarithm and exponential functions in terms of the Meijer's G-function by using [17, Eq. (8.4.6.5)] and [17, Eq. (8.4.3.1)], respectively. The resulting expression can be written as

$$\bar{\mathcal{C}} = \frac{\alpha}{(2\ln 2)e^{\kappa\mu}} \sum_{j=0}^{\infty} \frac{\mu^{\mu+2j}\kappa^j(1+\kappa)^{\mu+j}}{j!\Gamma(\mu+j)\bar{\gamma}^{\frac{\alpha}{2}(\mu+j)}} \int_0^{\infty} x^{\frac{\alpha}{2}(\mu+j)-1} \times G_{2,2}^{1,2}\left(x \middle| \begin{matrix} 1,1 \\ 1,0 \end{matrix}\right) G_{0,1}^{1,0}\left(\frac{\mu(1+\kappa)}{\bar{\gamma}^{\frac{\alpha}{2}}} x^{\frac{\alpha}{2}} \middle| \begin{matrix} - \\ 0 \end{matrix}\right) \mathrm{d}x, \quad (9)$$

in which the required integral can be evaluated by using [18] as (10), shown at the top of the next page. Again it is worth

[1]The Fox H-function is a generalized function that has become popular in performance analysis of wireless communication systems. Such a function is not readily available in software computation packages (e.g., MATHEMATICA or Matlab), but [19] has proposed an efficient and accurate approach in MATHEMATICA.

1089-7798 (c) 2018 IEEE. Personal use is permitted, but republication/redistribution requires IEEE permission. See http://www.ieee.org/publications_standards/publications/rights/index.html for more information.

This article has been accepted for publication in a future issue of this journal, but has not been fully edited. Content may change prior to final publication. Citation information: DOI 10.1109/LCOMM.2018.2878218, IEEE Communications Letters

$$\bar{\mathcal{P}}_e = \frac{A\alpha}{2\sqrt{\pi}e^{\kappa\mu}} \sum_{j=0}^{\infty} \frac{\mu^{\mu+2j}\kappa^j(1+\kappa)^{\mu+j}}{j!\Gamma(\mu+j)\left(B\bar{\gamma}\right)^{\frac{\alpha}{2}(\mu+j)}} H_{2,2}^{1,2}\left(\frac{\mu(1+\kappa)}{\left(B\bar{\gamma}\right)^{\frac{\alpha}{2}}}\middle|\begin{matrix}\left(1-\frac{\alpha}{2}(\mu+j),\frac{\alpha}{2}\right),\left(\frac{1}{2}-\frac{\alpha}{2}(\mu+j),\frac{\alpha}{2}\right)\\ (0,1),\left(-\frac{\alpha}{2}(\mu+j),\frac{\alpha}{2}\right)\end{matrix}\right). \quad (5)$$

$$\bar{\mathcal{C}} = \frac{\alpha}{2(\ln 2)e^{\kappa\mu}} \sum_{j=0}^{\infty} \frac{\mu^{\mu+2j}\kappa^j(1+\kappa)^{\mu+j}}{j!\Gamma(\mu+j)\bar{\gamma}^{\frac{\alpha}{2}(\mu+j)}} H_{2,3}^{3,1}\left(\frac{\mu(1+\kappa)}{\bar{\gamma}^{\frac{\alpha}{2}}}\middle|\begin{matrix}\left(-\frac{\alpha}{2}(\mu+j),\frac{\alpha}{2}\right),\left(1-\frac{\alpha}{2}(\mu+j),\frac{\alpha}{2}\right)\\ (0,1),\left(-\frac{\alpha}{2}(\mu+j),\frac{\alpha}{2}\right),\left(-\frac{\alpha}{2}(\mu+j),\frac{\alpha}{2}\right)\end{matrix}\right). \quad (10)$$

$$\epsilon_{\bar{P}_e} < \frac{A\alpha\mu^{\mu}(1+\kappa)^{\mu}e^{-\kappa\mu}}{2\sqrt{\pi}\Gamma(\mu)\left(B\bar{\gamma}\right)^{\frac{\alpha\mu}{2}}} {}_0F_1\left(;\mu;\frac{\mu^2\kappa(1+\kappa)}{\left(B\bar{\gamma}\right)^{\frac{\alpha}{2}}}\right) H_{2,2}^{1,2}\left(\frac{\mu(1+\kappa)}{\left(B\bar{\gamma}\right)^{\frac{\alpha}{2}}}\middle|\begin{matrix}\left(1-\frac{\alpha}{2}(\mu+p),\frac{\alpha}{2}\right),\left(\frac{1}{2}-\frac{\alpha}{2}(\mu+p),\frac{\alpha}{2}\right)\\ (0,1),\left(-\frac{\alpha}{2}(\mu+p),\frac{\alpha}{2}\right)\end{matrix}\right). \quad (13)$$

$$\epsilon_{\bar{C}} < \frac{\alpha\mu^{\mu}(1+\kappa)^{\mu}e^{-\kappa\mu}}{2(\ln 2)\Gamma(\mu)\bar{\gamma}^{\frac{\alpha\mu}{2}}} {}_0F_1\left(;\mu;\frac{\mu^2\kappa(1+\kappa)}{\bar{\gamma}^{\frac{\alpha}{2}}}\right) H_{2,3}^{3,1}\left(\frac{\mu(1+\kappa)}{\bar{\gamma}^{\frac{\alpha}{2}}}\middle|\begin{matrix}\left(-\frac{\alpha}{2}(\mu+p),\frac{\alpha}{2}\right),\left(1-\frac{\alpha}{2}(\mu+p),\frac{\alpha}{2}\right)\\ (0,1),\left(-\frac{\alpha}{2}(\mu+p),\frac{\alpha}{2}\right),\left(-\frac{\alpha}{2}(\mu+p),\frac{\alpha}{2}\right)\end{matrix}\right). \quad (14)$$

noting that although the derived analytical expression is given in terms of an infinite series, it converges rapidly and steadily after a few terms for a desired accuracy.

VI. Closed-form Bound for the Truncation Error

The expressions of the above-mentioned performance metrics are given in terms of infinite series. As aforementioned, they converge rapidly to accurate results after a few terms which depend on the value of the involved parameters to ensure acceptable truncation. In what follows, closed-form bounds for the truncation error of the derived series representations are provided.

A. Outage Probability

Using (2), the truncation of the outage probability after $p-1$ terms results to the following truncation error

$$\epsilon_{P_{\text{out}}} = \sum_{j=p}^{\infty} \frac{\mu^j\kappa^j}{j!\Gamma(\mu+j)e^{\kappa\mu}} \Upsilon\left(\mu+j, \frac{\mu(1+\kappa)}{\bar{\gamma}^{\frac{\alpha}{2}}}\gamma_{\text{th}}^{\frac{\alpha}{2}}\right). \quad (11)$$

By changing the summation index to $n = j - p$ in (11), and noting that $\Upsilon(a,x) < \Upsilon(a+1,x)$ followed by the use of the identities $(n+p)! = p!(p+1)_n$, $(1)_n = n!$, the definition ${}_1F_2(a_1;b_1,b_2;z) = \sum_{n=0}^{\infty}\frac{(a_1)_n}{(b_1)_n(b_2)_n}\frac{z^n}{n!}$, and some manipulations, the bound can be expressed as

$$\epsilon_{P_{\text{out}}} > \frac{\mu^p\kappa^p {}_1F_2\left(1;1+p,\mu+p;1\right)}{\Gamma(\mu+p)p!e^{\kappa\mu}} \Upsilon\left(\mu+p, \frac{\mu(1+\kappa)}{\bar{\gamma}^{\frac{\alpha}{2}}}\gamma_{\text{th}}^{\frac{\alpha}{2}}\right), \quad (12)$$

where ${}_1F_2\left(;;\right)$ is the generalized Hypergeometric function defined in [16, Eq. (9.14.1)] and $(a)_b = \frac{\Gamma(a+b)}{\Gamma(b)}$ is the Pochhammer symbol.

B. AER and Normalized Average Capacity

Using a similar approach, closed-form upper bounds for the truncation error of (5) and (10) are given by (13) and (14), respectively, shown at the top of this page, where ${}_0F_1\left(;;\right)$ is defined in [16, Eq. (9.14.1)].

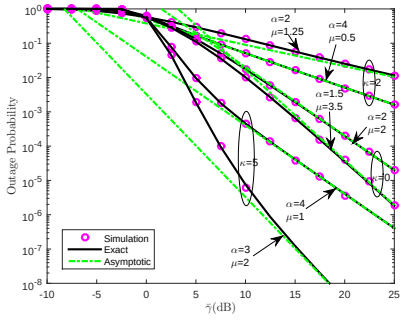


Fig. 1: Outage probability versus average SNR $\bar{\gamma}$ for several values of α, κ and μ.

VII. Numerical Results and Discussions

In this section, some representative numerical examples are presented to evaluate the effect of the fading parameters on the performance of the proposed system and channel models. Without loss of generality, we assume: $R_{\text{th}} = 1$ bit/s/Hz, and $A = \frac{1}{2}$ and $B = 1$ for BPSK modulation.

Fig. 1 shows the OP performance versus the average SNR for various values of the fading parameters α, κ and μ. It is evident that the exact curves, from (2), are in perfect agreement with the Monte Carlo simulations. In addition, it can be noted that the asymptotic curves accurately approximate the exact curves at high SNR. The asymptotic curves provide the diversity order of the underlying system. According to (3), the diversity order increases with either α, μ or both, which results in the decrease of the outage performance as illustrated in Fig. 1. This is further corroborated by noting that for fixed values of $\kappa = \{0, 2, 5\}$, the diversity gain changes when either α or μ varies, or when both vary.

Fig. 2 plots the average BER of the coherent BPSK modulation versus the average SNR for different values of α, κ and μ. Again, note the good match between the exact curves and the Monte Carlo simulations. Moreover, the curves for the

1089-7798 (c) 2018 IEEE. Personal use is permitted, but republication/redistribution requires IEEE permission. See http://www.ieee.org/publications_standards/publications/rights/index.html for more information.

This article has been accepted for publication in a future issue of this journal, but has not been fully edited. Content may change prior to final publication. Citation information: DOI 10.1109/LCOMM.2018.2878218, IEEE Communications Letters

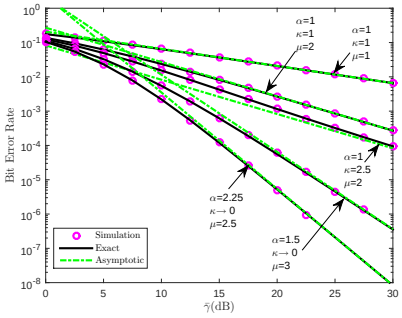


Fig. 2: Average BER versus average SNR $\bar{\gamma}$ for several values of α, κ and μ.

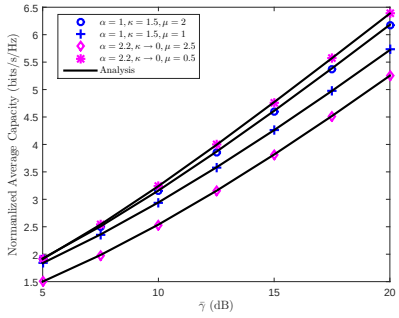


Fig. 3: Normalized Average Capacity versus average SNR $\bar{\gamma}$ for several values of α, κ and μ. The markers represent Monte Carlo simulations.

approximate BER are tight over the entire SNR regime, while the asymptotic curves well approximate the exact ones in the high SNR regime. As can be seen, the average BER decreases for an increase in the fading parameter μ (see the cases where $\mu = 1$ and $\mu = 2$ when $\alpha = 1$ and $\kappa = 1$). It can also be implied that this will be the case for an increase in the fading parameter α as attested by the diversity gain.

In Fig. 3, Monte Carlo simulations and theoretical results from (10) for the normalized average capacity are compared, and it is attested that both are in good agreement over the entire SNR regime. Also, it can be observed that for fixed α and κ values, the normalized average capacity varies with an increase in the fading parameter μ. Fig. 4 shows the relative errors with bound and truncation (pertaining to $\mathcal{P}_{\text{out}}$) versus the number of terms p when $\alpha = 1$, $\kappa = 2$, $\mu = 2$ and for various values of the average SNR. The relative error with the bound is given by $\frac{\epsilon_{P_{\text{out}}}}{\text{exact}}$, while the one due to truncation can be expressed as $\frac{|\text{exact}-\text{truncated}|}{\text{exact}}$, where the exact value is calculated via numerical integration and the truncated value is computed for various values of p using (2). For $\bar{\gamma} = 10$ dB and $\bar{\gamma} = 20$ dB, it can be noted that the relative errors with truncation and with bound are less than 10^{-5} for $p \geq 8$, which shows the tightness of the derived error bound after a few terms. Due to space limitation, the relative errors with truncation and bound for the AER and normalized average capacity are not presented.

VIII. Conclusion

In this letter, a comprehensive analytical framework for the performance evaluation of digital communication systems over

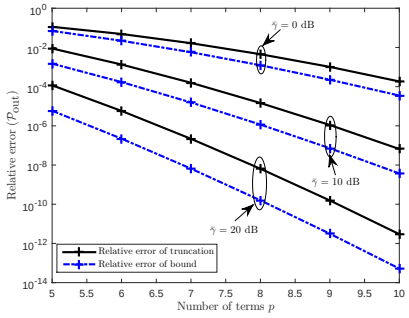


Fig. 4: Relative error versus the number of terms p for various average SNR values.

α-κ-μ fading channels has been presented in terms of OP, normalized average capacity and AER (valid for all coherent modulations). All the attained analytical results can definitely be used as a benchmark for future studies considering α-κ-μ fading model, in which a deeper performance analysis investigation is still in its infancy.

References

[1] M. K. Simon and M. -S. Alouini, *Digital Communication Over Fading Channels*, 2nd ed., John Wiley & Sons, 2000.

[2] M. D. Yacoub, "The α-μ distribution: A physical fading model for the Stacy distribution," *IEEE Trans. Veh. Technol.*, vol. 56, no. 1, pp. 27–34, Jan. 2007.

[3] ——, "The η-μ distribution and the κ-μ distribution,," *IEEE Antennas Propag. Mag.*,, vol. 49, no. 1, pp. 68–81, Feb. 2007.

[4] G. Fraidenraich and M. D. Yacoub, "The α-η-μ and α-κ-μ fading distributions," 2006, pp. 16–20, Manaus, Amazon, Brazil.

[5] R. Cogliatti and R. A. A. de Souza, "A near-100% efficient algorithm for generating α-κ-μ and α-η-μ variates," 2013, pp. 1–5, Las Vegas, NV, USA.

[6] M. D. Yacoub, "The α-η-κ-μ fading model," *IEEE Trans. Antennas Propag.*, vol. 64, no. 8, pp. 3597–3610, Aug. 2016.

[7] P. S. Bithas, N. C. Sagias, P. T. Mathiopoulos, G. K. Karagiannidis, and A. A. Rontogiannis, "On the performance anlysis of digital communications over generalized-K fading channels," *IEEE Commun. Lett.*, vol. 10, no. 5, pp. 353–355, May 2006.

[8] D. Morales-Jiménez and J. F. Paris, "Outage probability analysis for η-μ fading channels," *IEEE Commun. Lett.*, vol. 14, no. 6, pp. 521–523, Jun. 2010.

[9] D. B. da Costa and M. Yacoub, "Average channel capacity for generalized fading scenarios," *IEEE Commun. Lett.*, vol. 11, no. 2, pp. 949–951, Dec. 2007.

[10] ——, "Moment generating functions of generalized fading distributions and applications," *IEEE Commun. Lett.*, vol. 12, no. 2, pp. 112–114, Feb. 2008.

[11] A. M. Magableh and M. Matalgah, "Moment generating function of the generalized α-μ distribution with applications," *IEEE Commun. Lett.*, vol. 13, no. 6, pp. 411–413, Jun. 2009.

[12] O. S. Badarneh and and M. S. Aloqlah, "Performance analysis of digital communication systems over α-η-μ fading channels," *IEEE Trans. Veh. Technol.*, vol. 65, no. 10, pp. 7972–7981, Oct. 2016.

[13] E. Salahat and A. Hakam, "Performance analysis of α-η-μ and α-κ-μ generalized mobile fading channels," 2006, pp. 16–20, Berlin, Germany.

[14] X. Li, X. Chen, J. Zhang, Y. Liang, and Y. Liu, "Capacity analysis of α-η-κ-μ fading channels," *IEEE Commun. Lett.*, vol. 21, no. 6, pp. 1449–1452, Jun. 2017.

[15] A. A. dos Anjos, T. R. R. Marins, R. A. A. de Souza, and M. D. Yacoub, "Higher Order Statistics for the α-η-κ-μ fading model," *IEEE Trans. Antennas Propag.*, vol. 66, no. 6, pp. 3002–3016, Jun. 2018.

[16] I. S. Gradshteyn and I. M. Ryzhik, *Table of Integrals, Series, and Products*, 7th ed., San Diego, CA: Academic, 2007.

[17] A. P. Prudnikov, Y. A. Brychkov, and O. I. Marichev, *Integrals and Series, Vol. 3: More Special Functions*, Oxford University Press US.

[18] I. Wolfram Research. Meijer G-function. [Online]. http://functions.wolfram.com/07.34.21.0012.01.

[19] F. Yilmaz and M.-S. Alouini, "Product of the powers of generalized Nakagami-m variates and performance of cascaded fading channels," in *Proc. IEEE Global Telecommunications Conference (Globecom)*, 2009, pp. 1–8, Honolulu, Hawai, USA.

[20] J. Proakis, *Digital Communications*, 4th ed., New York: McGraw-Hill, 2001.

1089-7798 (c) 2018 IEEE. Personal use is permitted, but republication/redistribution requires IEEE permission. See http://www.ieee.org/publications_standards/publications/rights/index.html for more information.